J Membrane Biol (2011) 241:11–20
DOI 10.1007/s00232-011-9358-6

Characterization of TRPM8-Like Channels Activated by the Cooling Agent Icilin in the Macrophage Cell Line RAW 264.7

Sheng-Nan Wu · Pei-Yu Wu · Mei-Ling Tsai

Received: 3 February 2011 / Accepted: 11 March 2011 / Published online: 29 March 2011

Abstract Icilin is recognized as a chemical agonist of nociceptors and can activate TRPM8 channels. However, whether this agent has any effects on immune cells remains unknown. In this study, the effects of icilin on ion currents were investigated in RAW 264.7 murine macrophage-like cells. Icilin (1–100 μM) increased the amplitude of non-selective (NS) cation current (I_{NS}) in a concentration-dependent manner with an EC_{50} value of 8.6 μM. $LaCl_3$ (100 μM) or capsazepine (30 μM) reversed icilin-induced I_{NS}; however, neither apamin (200 nM) nor iberiotoxin (200 nM) had any effects on it. In cell-attached configuration, when the electrode was filled with icilin (30 μM), a unique population of NS cation channels were activated with single-channel conductance of 158 pS. With the use of a long-lasting ramp pulse protocol, increasing icilin concentration produced a left shift in the activation curve of NS channels, with no change in the slope factor of the curve. The probability of channel opening enhanced by icilin was increased by either elevated extracellular Ca^{2+} or application of ionomycin (10 μM), while it was reduced by BAPTA-AM (10 μM). Icilin-stimulated activity is associated with an increase in mean open time and a reduction in mean closed time. Under current-clamp conditions, icilin caused membrane depolarization. Therefore, icilin interacts with the TRPM8-like channel to increase I_{NS} and depolarizes the membrane in these cells.

Keywords Icilin · Nonselective cation channel · RAW 264.7 macrophage · Membrane potential

Introduction

Transient receptor potential melastatin 8 (TRPM8 or *trp-p8*), a member of the melastatin subfamily, has been recognized as a cold receptor and functions as a transducer of innocuous cold stimuli in the somatosensory system (McKemy et al. 2002). It is a ligand-gated cation channel, with moderate to high selectivity of Ca^{2+} ions. TRPM8 is activated by chemicals that elicit sensations of cold, with an activation temperature of ~25–28°C (Harteneck 2005; Wang and Woolf 2005). Mice lacking TRPM8 were noted to display deficiencies in response to icilin, menthol and noxious cold (Colburn et al. 2007). Aside from its restricted localization in sensory neurons, the human ortholog of TRPM8 is expressed in the testis, bladder urothelium, prostate tissue, breast cancer cells and neuroendocrine tumor cells (Chodon et al. 2010; Mergler et al. 2007; Valero et al. 2011; Zholos 2010). It is also noted that activation of the TRPM8 variant in human lung epithelial cells might cause increased expression of several cytokine and chemokine genes (Sabnis et al. 2008). However, the function of TRPM8 in nonneuronal tissues, particularly in immune cells, is largely unknown, although it is reported to be functionally expressed in the vasculature (Johnson et al. 2009; Zholos 2010).

RAW 264.7 cells, a macrophage-like, Abelson leukemia virus–transformed cell line, are known to possess the characteristics of macrophages. They have attracted

Electronic supplementary material The online version of this article (doi:10.1007/s00232-011-9358-6) contains supplementary material, which is available to authorized users.

S.-N. Wu (✉) · P.-Y. Wu · M.-L. Tsai
Department of Physiology, National Cheng Kung University Medical College, No. 1, University Road, Tainan 70101, Taiwan
e-mail: snwu@mail.ncku.edu.tw

S.-N. Wu · P.-Y. Wu · M.-L. Tsai
Institute of Basic Medical Sciences, National Cheng Kung University Medical College, Tainan, Taiwan

growing interest as a suitable model for studies of functional activities, signaling cascade and morphological characteristics in macrophages (Channon and Leslie 1990; Kuo et al. 2005; Pan et al. 2008). Macrophages and neutrophils are reported to express TRPM2 or TRPV2, and elevation of intracellular Ca^{2+} through activation of this channel may be an important part of respiratory burst and may regulate other aspects of the inflammatory response, including cytokine production (Perraud et al. 2004; Miller 2006; Yamashiro et al. 2010). Together with TRPV3 and TRPV4, TRPV2 has been characterized as a heat or warmth thermosensor (Tominaga and Caterina 2004).

Icilin, a synthetic chemical compound, contains hexacyclic aromatic rings in its structure and is known to activate TRPM8 channels with high efficacy and potency (Chuang et al. 2004; McKemy et al. 2002). There is growing evidence that the magnitude of TRPM8-encoded currents activated by menthol or icilin is involved in the inflammation-induced sensitivity to cold (Colburn et al. 2007; Sabnis et al. 2008). It has long been recognized that macrophages are activated in the inflammatory process. However, the issue of how icilin can interact with ion currents in macrophages remains elusive. In this study, we provide evidence that chemical stimulation of RAW 264.7 cells by icilin can interact with a large-conductance nonselective (NS) cation channel to increase the amplitude of NS cation current (I_{NS}) and to depolarize the membrane.

Materials and Methods

Cell Preparation

The murine macrophage cell line RAW 264.7 was obtained from the American Type Culture Collection (TIB-71; Manassas, VA). Cells were routinely grown in Dulbecco's modified Eagle medium supplemented with 10% heat-inactivated fetal bovine serum, 100 U/ml penicillin and 100 μg/ml streptomycin (Kuo et al. 2005). They were maintained in a 95% air and 5% CO_2 humidified atmosphere at 37°C. Cell viability was often assessed by the trypan blue dye-exclusion test. To observe cell growth, a Nikon Eclipse Ti-E inverted microscope (Li Trading, Taipei, Taiwan) equipped with a 5-megapixel cooled digital camera was used. The digital camera was connected to a personal computer controlled by NIS-Elements BR3.0 software (Nikon, Kanagawa, Japan). Some cells displayed an irregular form with accelerated spreading and formation of pseudopodia (Fig. 1). Treatment of RAW 264.7 cells with lipopolysaccharide (0.5 μg/ml) for 2 days was found to significantly increase the number of cells with such morphologic changes (Pan et al. 2008). For subculturing, cells were trypsin-dissociated and passaged every 2–3 days.

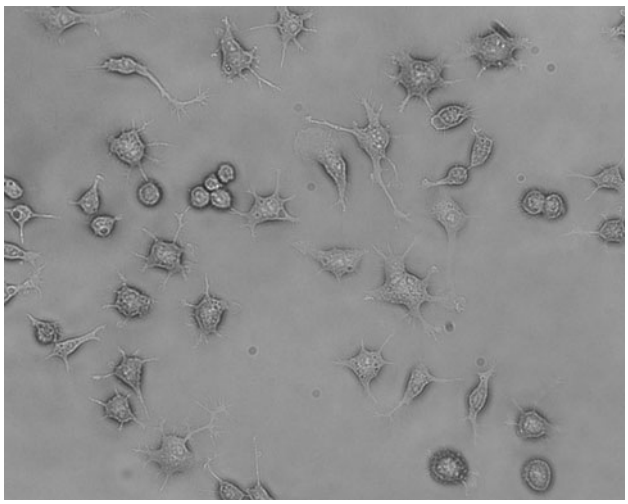

Fig. 1 Morphology of RAW 264.7 macrophages. Living cells were photographed under phase contrast (×200). Notably, a few cells displayed an irregular form with pseudopodia

Electrophysiological Measurement

Before each experiment, RAW 264.7 cells were dissociated and an aliquot of the cell suspension was subsequently transferred to a recording chamber mounted on the stage of an inverted DM-IL microscope (Leica, Wetzlar, Germany). Cells were immersed at room temperature (23 ± 2°C, $n = 12$) in normal Tyrode's solution. Patch pipettes were pulled from Kimax-51 glass capillaries (Kimble, Vineland, NJ) using a two-stage electrode puller (PP-830; Narishige, Tokyo, Japan), and their tips were fire-polished with an MF-83 microforge (Narishige). The pipette had a resistance of 3–5 MΩ when immersed in normal Tyrode's solution. Ion currents were measured with glass pipettes in standard patch-clamp technique using an RK-400 amplifier (Bio-Logic, Claix, France) (Wu et al. 2003, 2008). All potentials were corrected for liquid junction potential, which develops at the tip of the electrode when the composition of the internal solution differs from that in the bath.

Data Recording and Analyses

Data were stored online in a TravelMate-6253 laptop computer (Acer, Taipei, Taiwan) at 10 kHz through a Digidata-1322A interface (Molecular Devices, Sunnyvale, CA). The interface device was equipped with an Adaptec (Milpitas, CA) SlimSCSI card via a PCMCIA slot and controlled by pCLAMP 9.2 (Molecular Devices). Current signals were low-pass-filtered at 1 or 3 kHz. pCLAMP-generated voltage-step protocols were used to evaluate the current–voltage (I–V) relationships for ion currents (e.g., I_{NS}). Signals were analyzed using Origin 8.0 (OriginLab, Northampton, MA) or custom-made macros built in Excel

2007 spreadsheet running under Windows-7 (Microsoft, Redmond, WA).

To calculate the concentration-dependent increase of icilin on the amplitude of I_{NS}, each cell was held at −50 mV, ramp pulses from −80 to +30 mV were applied and current amplitudes at −60 mV were measured during exposure to icilin (1–100 μM). The I_{NS} amplitude during cell exposure to 100 μM icilin was taken as 1.0. The concentration required to stimulate 50% of current amplitude was then determined by means of a Hill function:

$$\text{Relative amplitude} = \frac{E_{\max} \times [C]^{n_H}}{\text{EC}_{50}^{n_H} + [C]^{n_H}}$$

where $[C]$ is the concentration of icilin; EC_{50} and n_H are the concentration required for a 50% stimulation and the Hill coefficient, respectively; and $E_{\max}$ is the maximal increase in current amplitude caused by icilin.

Single-Channel Analyses

Single-channel currents recorded from RAW 264.7 cells were analyzed using pCLAMP 10.2 software (Molecular Devices). Single-channel amplitudes were often determined by fitting gaussian distributions to the amplitude histograms of the closed and open states. Channel activity was defined as $N \cdot P_O$, a product of channel number (N) and open probability (P_O). Single-channel conductance was calculated by a linear regression using mean values of current amplitudes measured at different potentials. Open and closed lifetime distributions were fitted with logarithmically scaled bin width. Origin 8.0 was used for fitting of experimental data.

To determine the effect of icilin on the activation curve of NS channels, ramp pulses from −30 to +50 mV over a 1-s period were applied to the patch. The activation curve was calculated by averaging current traces in response to 20 voltage ramps and subsequently by dividing each point of the mean current by unitary amplitude for each potential after leakage currents were corrected (Carl and Sanders 1990). The activation curves obtained in the presence of 3 and 30 μM icilin were then fitted with the Boltzmann equation:

$$\text{Relative } N \cdot P_O = \frac{n_P}{1 + \exp[-(V - a)/b]},$$

where n_P is the maximal relative $N \cdot P_O$, b is the slope factor of the voltage-dependent activation (i.e., change in the potential required to result in an e-fold increase in the activation) and a is the voltage at which there is half-maximal activation. Because the linearization procedure causes adverse effects on the determination of the best-fit parameter values, nonlinear least-squares fitting was made in the Solver-add-in bundled with Microsoft Excel 2007 (Kemmer and Keller 2010).

The data of macroscopic or single-channel currents are presented as means ± SEM, with sample sizes (n) indicating the number of cells examined. Paired or unpaired Student's t-test and one-way analyses of variance with a least-significance difference method for multiple-group comparisons were used for the statistical evaluation of differences among means. To evaluate the sum of squared residuals (SSR), 99% confidence intervals were estimated with the use of Fisher's F distribution. Differences were considered statistically significant at $P < 0.05$.

Drugs and Solution

Icilin (AG-3-5, 3,4-dihydro-3-[2-hydroxyphenyl]6-[3-nitrophenyl]-[1H]-pyrimidin-2-one, 1-[2-hydroxyphenyl]-4-[3-nitrophenyl]-1,2,3,6-tetrahydropyrimidin-2-one) and nonactin were obtained from Tocris Cookson (Bristol, UK), DL-menthol and lipopolysaccharide were from Sigma-Aldrich (St. Louis, MO), ionomycin and 1,2-bis(2-aminophenoxymethyl)ethane-*N*,*N*,*N*′,*N*′-tetraacetic acid tetrakis (acetoxymethyl ester) (BAPTA-AM) were from Invitrogen (Taipei, Taiwan), iberiotoxin and apamin were from Alomone Labs (Jerusalem, Israel) and capsazepine was from Enzo (Plymouth Meeting, PA). Icilin was prepared as 10–30 mM stock solutions in dimethyl sulfoxide (DMSO) and added to bath solution at the indicated final concentration. All culture media, fetal calf serum, L-glutamine, trypsin/EDTA and penicillin–streptomycin were obtained from Invitrogen. All other chemicals were commercially available and of reagent grade. Deionized water used in all experiments was made from a Milli-Q water purification system (Millipore, Bedford, MA).

The composition of normal Tyrode's solution used in this study was as follows (in mM): NaCl 136.5, KCl 5.4, $CaCl_2$ 1.8, $MgCl_2$ 0.53, glucose 5.5 and HEPES-NaOH buffer 5.5 (pH 7.4). To record icilin-induced I_{NS}, the patch pipette was filled with the following solution (in mM): Cs-aspartate 130, CsCl 20, $MgCl_2$ 1, Na_2ATP 3, Na_2GTP 0.1, EGTA 0.1 and HEPES-KOH buffer 5.5 (pH 7.2). In experiments designed to evaluate cation selectivity of icilin-elicited I_{NS}, Cs^+ was replaced with equimolar concentrations of Na^+, K^+ or $NMDG^+$. To determine anion selectivity, aspartate was replaced with Cl^-. To measure membrane potential or K^+ current, Cs^+ ions inside the pipette solution were replaced with equimolar K^+ ions and the pH was adjusted to 7.2 with KOH. Ca^{2+}-free solution used was a solution where $CaCl_2$ was not added.

Results

Effect of Icilin on I_{NS} in RAW 264.7 Cells

In the initial set of experiments, a whole-cell configuration was used to investigate the electrical properties of

macroscopic I_{NS} in these cells. Cells were bathed in Ca^{2+}-free Tyrode's solution, and the recording pipette was filled with a Cs^+-containing pipette solution. When the cell was held at −50 mV, ramp pulses from −80 to +20 mV with a duration of 1 s were applied. As shown in Fig. 2a, when cells were exposed to icilin, the amplitude of I_{NS} was greatly increased. For example, at the level of −60 mV, icilin (30 μM) significantly increased the amplitude of I_{NS} from 45 ± 9 to 302 ± 22 pA ($n = 8$). After washout of the compound, the current amplitude returned to 187 ± 13 pA ($n = 5$). When Cs^+ ions in the pipette solution were replaced with equimolar concentrations of Na^+, K^+ or $NMDG^+$, this current could still be induced by icilin (30 μM). The relationship between the icilin concentration and the relative amplitude of I_{NS} was constructed (Fig. 2b). The half-maximal concentration required for its stimulation of I_{NS} was 8.6 ± 0.9 μM ($n = 12$). In the SSR plot shown in the inset of Fig. 2b, a horizontal line at SSR = 0.344 was made to determine the two EC_{50} values. For a 99% confidence interval, the lower and upper values were 5.84 and 12.94 μM, respectively. Because there was a steep slope on both sides of the minimum, the value for relative amplitude of I_{NS} was determined with high confidence. Similarly, menthol (1 mM) was able to increase the I_{NS} amplitude in these cells. Subsequent application of 100 μM $LaCl_3$ or 30 μM capsazepine reversed the increased amplitude of I_{NS} induced by icilin (30 μM) (Fig. 2c). In contrast, the inhibitors of Ca^{2+}-activated K^+ (K_{Ca}) channels, such as iberiotoxin (200 nM) and apamin (200 nM), produced no effects on icilin-stimulated I_{NS} (Fig. 2c). Therefore, results from these observations reflect that, in RAW 264.7 cells, icilin has a stimulatory effect on I_{NS}, rather than on K_{Ca}, currents (Wondergem and Bartley 2009).

Electric Properties of Icilin-Induced NS Channels Recorded from RAW 264.7 Cells

The icilin-stimulated increase of I_{NS} described above could be due to either the increased open probability, an increase in the number of active channels or changes in the channel gating. The effects of this compound on the activity of NS channels were further investigated. In these experiments, RAW 264.7 cells were bathed in Ca^{2+}-free solution, and single-channel recordings with cell-attached configuration were conducted when the recording pipette was filled with a Cs^+-containing solution in which 30 μM icilin was included. The reason that Ca^{2+}-free solution was used in this set of experiments is that the activity of K_{Ca} channels expressed in RAW 264.7 cells might be contaminated. In cell-attached patches from the recording pipette filled without icilin, little or no activity of NS channels was observed at −70 mV, a value that is near the resting potential of cells. However, when the recording pipette was filled with 30 μM icilin, there was a drastic increase in NS-channel activity at the same level (Fig. 3). The single-channel amplitude at −150 mV was 24.7 ± 2.1 pA ($n = 8$). Figure 3c illustrates an ohmic *I–V* relationship of NS channels in RAW 264.7 cells. A fit of the data using a linear *I–V* relationship yielded the single-channel conductance and reversal potential of 158 ± 10 pS and −5.8 ± 1.1 mV ($n = 9$), respectively. A plot of SSR vs. single-channel conductance of icilin-induced NS channels is shown in the inset of Fig. 3c. The steep slope on both sides of the minimum indicates that the value of single-channel conductance is determined with high confidence. The values for these channels in the presence of 30 μM icilin did not differ significantly from those obtained in the pipette filled with 3 μM icilin (156 ± 11 pS and −5.9 ± 1.2 mV, $n = 6$). The results indicate that this compound increases the activity of NS channels observed in RAW 264.7 cells in a membrane-delimited manner. Similarly, in inside–out configuration, when icilin (30 μM) was applied to the internal surface of the detached patch, the activity of NS channels was also activated.

Effect of Icilin on Voltage-Dependent Activation of NS Channels from RAW 264.7 Cells

Experiments were next carried out to examine the voltage dependence of icilin-induced activity of NS channels with the use of long-lasting ramp pulses (Fig. 4). In this set of experiments, cells were bathed in Ca^{2+}-free solution and single-channel recordings with cell-attached configuration were conducted. Figure 4a shows a representative graph of the effect of icilin on the activity of NS channels in the recording pipette filled with 30 μM icilin. Icilin-induced NS-channel activity observed in RAW 264.7 cells displayed outward rectification. There appeared to be synchronized openings of several channels, particularly at the level of depolarizing potentials. The activation curves of NS channels in the electrodes filled with 3 and 30 μM icilin are depicted in Fig. 4b. In these experiments, the activation curve of NS channels was obtained by the use of a consecutive upsloping ramp protocol in which each pulse was digitally generated and applied from −30 to +50 mV with a duration of 1 s at a rate of 0.05 Hz. The plots of the probability of channel openings as a function of membrane potential were constructed and fitted with the Boltzmann distribution as described in Materials and Methods. In the electrode filled with 3 μM icilin $n_P = 1.61 \pm 0.11$, $a = 24 \pm 3$ mV and $b = 11.1 \pm 1.9$ mV ($n = 6$), and in that with 30 μM icilin $n_P = 3.62 \pm 0.41$, $a = 8 \pm 1$ mV and $b = 9.7 \pm 1.2$ mV ($n = 6$). In light of these data, increasing the icilin concentration from 3 to 30 μM caused an approximately 16-mV leftward shift in voltage-dependent

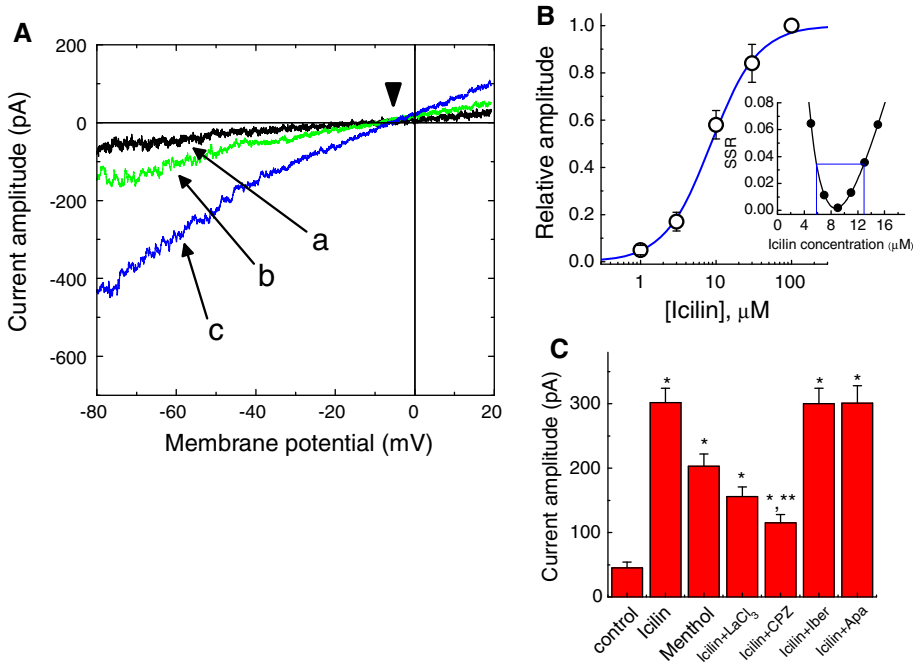

Fig. 2 Activation of nonselective cation current (I_{NS}) by icilin in RAW 264.7 macrophages. In these experiments, cells were bathed in Ca^{2+}-free Tyrode's solution and the patch pipette was filled with a Cs^{+} solution. **a** Superimposed current traces in response to voltage ramp pulses. The cell was held at −50 mV and ramp pulses from −80 to +20 mV with a duration of 1 s were applied at a rate of 0.01 Hz. *a*, control; *b*, 3 μM icilin; *c*, 30 μM icilin. *Arrowhead* indicates the level of reversal potential (−5.7 mV). **b** The relationship between the relative amplitude of I_{NS} and the icilin concentration. At the level of −60 mV, current amplitude in the presence of 100 μM icilin was considered to be 1.0. The values for EC_{50}, Hill coefficient and maximal relative amplitude of I_{NS} during cell exposure to icilin were 8.6 μM, 1.4 and 1.0, respectively. Each point represents the mean ± SEM (n = 7–12). *Inset* shows confidence assessment of best-fit parameter values. The parameter range corresponds to the approximate 99% confidence intervals. *Blue/thin line* marks parameter value (i.e., EC_{50}) at which the sum of squared residuals (SSR) amounts to 344.56%^{2}. **c** Bar graph showing summary of the effect of icilin (30 μM), menthol (1 mM), icilin plus $LaCl_3$ (100 μM), icilin plus capsazepine (*CPZ*, 30 μM), icilin plus iberiotoxin (*Iber*, 200 nM) and icilin plus apamin (*Apa*, 200 nM) on the amplitude of I_{NS} in RAW 264.7 cells. In the experiments with icilin plus each agent (e.g., $LaCl_3$, capsazepine, iberiotoxin and apamin), each compound was applied after the addition of icilin (30 μM). Each bar represents the mean ± SEM (n = 6–12). *Significantly different from control and **from icilin (30 μM) alone group (Color figure online)

activation of NS channels, despite its ability to increase the probability of channel openings. However, there was no significant change in the slope factor (i.e., *b* value) of the activation curve in RAW 264.7 cells. It is clear that in addition to the increased open probability, icilin can modify the voltage dependence of these channels in these cells.

Effect of Internal Ca^{2+} Concentration on Icilin-Stimulated NS-Channel Activity in RAW 264.7 Cells

Whether the icilin-induced increase in the activity of NS channels is associated with internal Ca^{2+} concentration was also studied. In these experiments, with cell-attached patches, the recording pipettes were filled with 30 μM icilin and cells were bathed in Ca^{2+}-free Tyrode's solution. As shown in Fig. 5a, when extracellular Ca^{2+} was elevated to 1.8 mM, the probability of channel openings induced by icilin was progressively increased. Figure 5b shows a summary of data on the effect of ionomycin or BAPTA-AM on icilin-stimulated activity of NS channels in RAW 264.7 cells. Ionomycin is a Ca^{2+} ionophore, while BAPTA-AM is a chelator of intracellular Ca^{2+}. However, in another set of experiments, cell-attached recordings with no inclusion of icilin inside the pipette showed that addition of ionomycin (10 μM) into the bath had no effect on channel activity. The results show that ionomycin (10 μM) can potentiate icilin-induced channel activity, while BAPTA-AM (10 μM) attenuates it. Moreover, the activity of K_{Ca} channels was not involved in the icilin-stimulated effect observed in these experiments. However, nonactin (10 μM), a neutral ionophore, had no effect on icilin-induced activity (data not shown). Therefore, it is clear from these data that icilin-stimulated NS-channel activity in these cells is closely linked to the level of intracellular Ca^{2+}.

Effect of Icilin on Kinetic Behavior of NS Channels in RAW264.7 Cells

The effect of icilin on the kinetic behavior of NS channels was further analyzed. As shown in Fig. 6, open- and

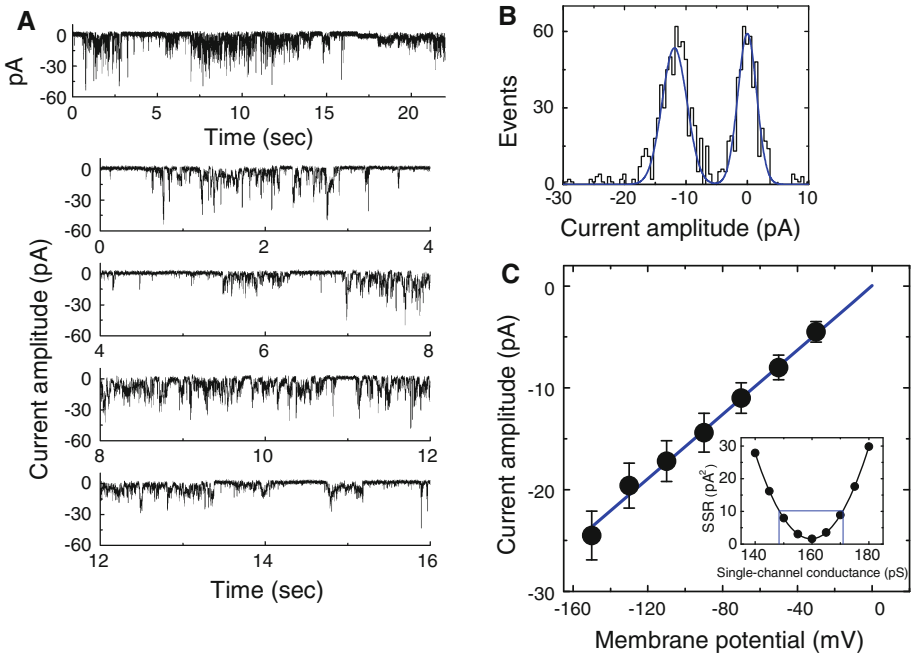

Fig. 3 Stimulatory effect of icilin on the activity of nonselective (NS) cation channels recorded from RAW 264.7 cells. Experiments were conducted in Ca^{2+}-free Tyrode's solution and cell-attached configuration and the recording pipette was filled with icilin (30 μM). Holding potential was set at −70 mV. **a** Original current traces obtained during exposure to 30 μM icilin. The lower part in **a** shows current traces obtained in an expanded time scale corresponding to those in the uppermost part of **a**. Downward deflection shown in this and the following figures indicates the opening events of the channel. **b** Amplitude histogram of icilin-induced NS channels in a RAW 264.7 cell. **c** *I–V* relationship of icilin-induced NS channels. The single-channel conductance of a unitary inward current was calculated to be 158 pS, with a reversal potential of −5.8 mV. *Inset* shows confidence assessment of best-fit parameter value. The range of single-channel conductance corresponds to the approximate 99% confidence intervals. *Blue/thin line* marks parameter value (i.e., single-channel conductance) at which the sum of squared residuals (SSR) amounts to 10.18 pA^2 (Color figure online)

closed-time histograms of NS channels at the level of −80 mV can be fitted by one- and two-exponential curves. The time constants of the open-time histogram in the presence of 3 and 30 μM icilin were 1.9 ± 0.3 and 3.5 ± 0.6 ms ($n = 6$), respectively. The time constants for the fast and slow components of the closed-time histogram in the presence of 3 μM icilin were 5.6 ± 0.8 and 35.1 ± 1.3 ms ($n = 6$), respectively, while those in the presence of 30 μM icilin were significantly reduced to 3.2 ± 0.7 and 28.7 ± 1.1 ms ($n = 6$), respectively. Therefore, it is clear that increasing the icilin concentration can cause a lengthening of mean open and a shortening of mean closed times in these cells.

Effect of Icilin on Resting Potential in RAW 264.7 Cells

In the final set of experiments, the effect of icilin on membrane potential was studied. Cells were bathed in normal Tyrode's solution containing 1.8 mM $CaCl_2$, and the recording pipette was filled with a K^+-containing solution. This type of macrophage had a resting membrane potential of −58 ± 6 mV ($n = 17$) under our current-clamp conditions. As shown in Fig. 7, application of icilin progressively caused membrane depolarization. During cell exposure to icilin (30 μM), the cell was depolarized to −18 ± 6 mV from a control value of −58 ± 5 mV ($n = 8$). After washout of icilin, the resting potential returned to −38 ± 6 mV ($n = 6$). In the continued presence of icilin (30 μM), neither iberiotoxin (200 nM) nor apamin (200 nM) caused any effect on changes in membrane potential. However, a further application of $LaCl_3$ (100 μM) reversed icilin-induced membrane depolarization (data not shown). The results suggest that the icilin-induced change in membrane polarization is associated with its activation of I_{NS} in RAW 264.7 cells.

Discussion

The major findings of this study are as follows. First, icilin, a chemical cooling agent, was effective at increasing the amplitude of I_{NS} in RAW 264.7 macrophage-like cells. Second, icilin activated a population of NS channels. As the icilin concentration was increased, the increased channel activity was accompanied by a shift of the steady-state activation toward a less depolarized range. Third, increasing the icilin concentration elevated the mean open

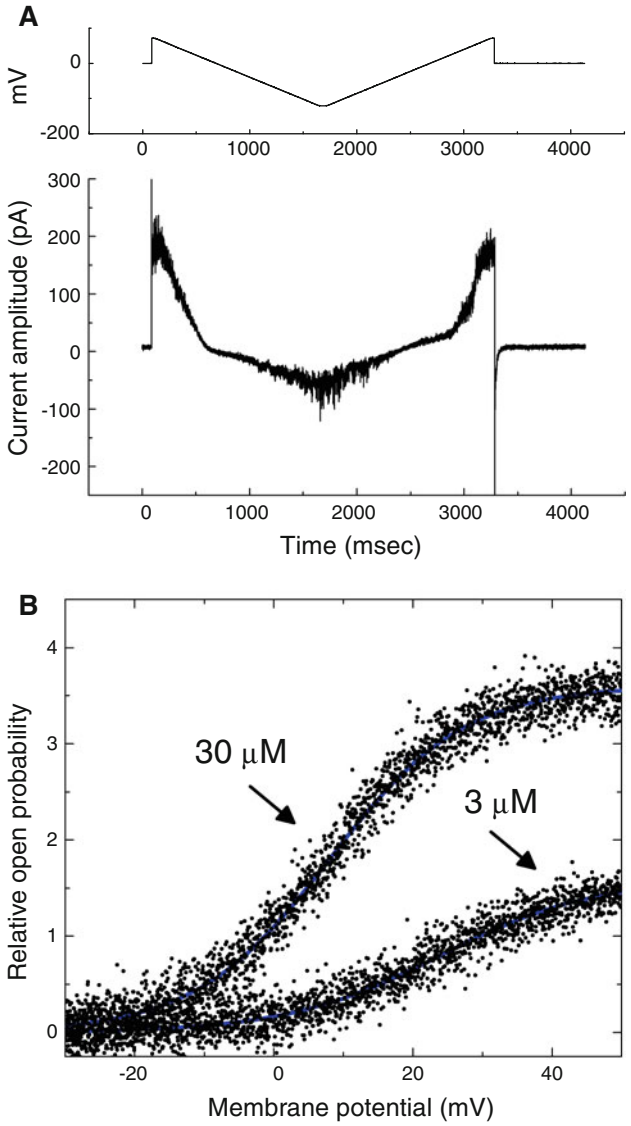

Fig. 4 Voltage dependence in icilin-induced activity of nonselective (NS) channels recorded from RAW 264.7 cells. **a** Original current trace elicited by long-lasting ramp pulse ranging between −120 and +70 mV with a duration of 3 s. The experiment was conducted in a recording pipette filled with 30 μM icilin. The upper part indicates the voltage protocol used. No leak compensation was made in this record. **b** Relationship between the open probability of NS channels and membrane potential in the electrode filled with 3 or 30 μM icilin. The activation curves were obtained when the ramp pulses were applied from −30 to +50 mV with a duration of 1 s. *Blue/smooth lines* represent the best fit to Boltzmann function as described under Materials and Methods (mean ± SEM, $n = 6$–9 for each point) (Color figure online)

time and reduced the mean closed time of the channels, thereby leading to an increase in channel open probability. Fourth, application of icilin caused membrane depolarization in these cells. The stimulatory effect of icilin on endogenous NS channels could be an important mechanism underlying icilin-induced action in macrophages if similar results occur in vivo.

A previous study showed the ability of menthol, another cooling agent, to stimulate the activity of large-conductance K_{Ca} channels in human glioblastoma cells (Wondergem and Bartley 2009). In our study, neither iberiotoxin nor apamin caused any effects on icilin-stimulated I_{NS}; however, $LaCl_3$ or capsazepine was effective at reversing the icilin-induced increase of I_{NS}. Therefore, the results excluded the possibility that icilin increased the probability of channel openings through activation of K_{Ca} channels in RAW 264.7 cells. The inability of iberiotoxin or apamin to reverse icilin-induced membrane depolarization is also consistent with these findings.

The amplitude of macroscopic I_{NS} enhanced by icilin was believed to be primarily due to an increase in channel open probability accompanied by both increased open dwell time and decreased closed dwell time, which is consistent with a recent study in TRPM8-expressing HEK293 cells (Fernández et al. 2011). Moreover, as the icilin concentration was elevated, no discernible change in the slope factor of the activation curve of its NS channels was seen. The results indicate that the stimulatory effect of icilin on NS channels in RAW 264.7 cells is not mediated by a direct effect on the voltage sensor per se and that its binding site may lie outside of the transmembrane field around the channel.

It was found that icilin stimulated the activity of NS channels to a greater magnitude when intracellular Ca^{2+} with either elevated extracellular Ca^{2+} or application of ionomycin was elevated. Further application of BAPTA-AM, an intracellular Ca^{2+} chelator, reversed the icilin-stimulated activity of NS channels. The results led us to suggest that, consistent with previous studies (Hui et al. 2005; Mahieu et al. 2010; Sherkheli et al. 2010), the activation by this compound of these channels is dependent on the level of intracellular Ca^{2+}. Both increased open and decreased closed times caused by icilin are likely to be associated with enhanced Ca^{2+} sensitivity of the channel. Therefore, this compound may bind to TRPM8-like channels at sites that are important for channel gating and are coupled to Ca^{2+} binding sites.

Previous studies showed that the sensitivity of TRPM8 to icilin depended on residues N799, D802 and G805, located in the cytoplasmic loop connecting TM2 and TM3 and within TM3 of rat TRPM8 (Chuang et al. 2004). However, in our study, the ability of icilin (30 μM) applied to the internal leaflet of the detached patch to activate NS-channel activity measured in the inside–out configuration was found to be similar to that in the cell-attached configuration, when the electrode was filled with the same concentration of icilin. The finding that the stimulatory effect of this cooling agent on NS channels in RAW 264.7 cells is not related to the sidedness of the membrane appeared to be different from previous studies (Chuang

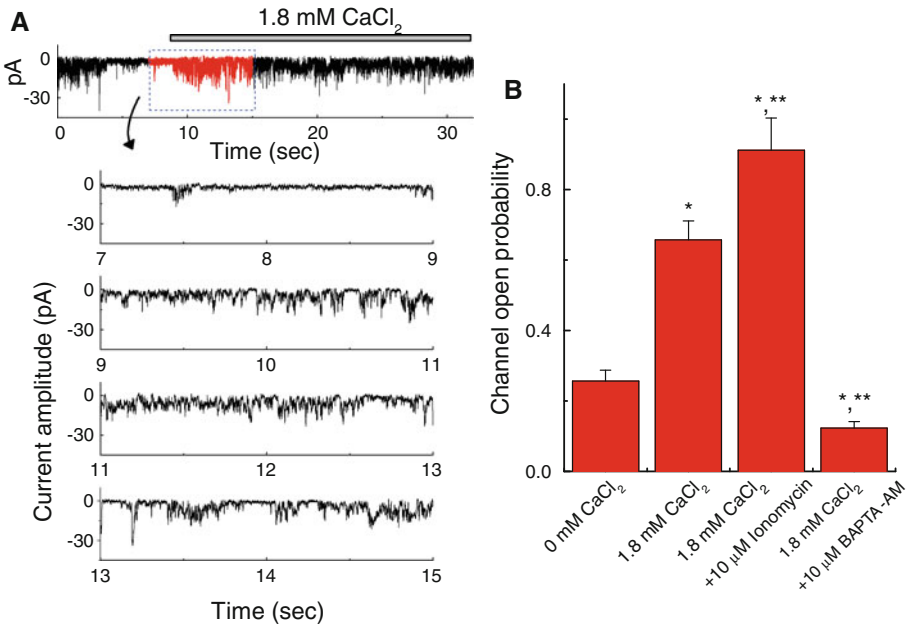

Fig. 5 Effects of extracellular Ca^{2+}, ionomycin and BAPTA-AM on the activity of icilin-induced nonselective (NS) channels in RAW 264.7 cells. **a** Original current traces showing the effect of extracellular Ca^{2+} on the activity of icilin-induced channels. In these experiments, cells were bathed in Ca^{2+}-free Tyrode's solution. Holding potential was set at −70 mV. *Horizontal bar* shown above indicates the application of 1.8 mM $CaCl_2$. The lower parts in **a** showing current traces obtained at an expanded scale correspond to that appearing in the uppermost part of **a** (*dashed box*). **b** Bar graph showing summary of the effect of extracellular Ca^{2+} (1.8 mM), ionomycin (10 μM) and BAPTA-AM (10 μM) on icilin-induced activity of NS channels in RAW 264.7 cells. Each bar represents the mean ± SEM (n = 8–11). *Significantly different from control (i.e., in the presence of Ca^{2+}-free Tyrode's solution) and **from the group in the presence of extracellular Ca^{2+} (1.8 mM) (Color figure online)

et al. 2004). Our results suggest that icilin is lipid-soluble and able to reach the binding site when it is applied extracellularly during cell-attached recordings. Different concentrations of membrane phospholipid (e.g., phosphatidylinositol 4,5-bisphosphate) might also contribute to the effect of icilin observed in this study (Zakharian et al. 2010). Moreover, the result that icilin-enhanced I_{NS} partially recovered after washout of this agent makes it unlikely that this agent can covalently bind to the channel.

From the *I–V* relationship of the unitary currents, icilin-elicited NS channels in RAW 264.7 cells were calculated to yield a single-channel conductance of 158 ± 10 pS (n = 9) at negative membrane potentials and appeared to be nonselective among monovalent cations. However, this value seemed to be greater than that of TRPM8 channels expressed in human embryonic kidney cells (Fernández et al. 2011; Hui et al. 2005) and reconstituted in planar lipid bilayers (Zakharian et al. 2010). Moreover, based on the excluded-volume equation (Sabovcik et al. 1995), the pore size created by the presence of icilin in RAW 264.7 cells was numerically estimated to be at least as large as 29.8 Å in diameter (see supplementary material).

A unique population of endogenous NS channels activated by icilin in RAW 264.7 cells shares similar characteristics in TRPM8 channels expressed in human embryonic kidney tsa-201 and in human IMR32 neuroblastoma cells (Hui et al. 2005; Louhivuori et al. 2009) and reconstituted in planar lipid bilayer (Zakharian et al. 2010). A concentration-dependent increase in the amplitude of I_{NS} with an EC_{50} value of 8.6 μM was observed in this study. These results suggest that the TRPM8-like channel expressed in macrophages may be an important target for the action of this compound and other TRPM8 antagonists (Parks et al. 2011). It is also necessary to elucidate their characteristics and physiological/pathophysiological function because, with the very large conductance described herein, opening of single channels can depolarize the cell membrane and lead to significant changes in the function of macrophages like RAW 264.7 cells. A previous study indeed demonstrated the presence of a functional TRPM8 variant in lung epithelial cells (Sabnis et al. 2008). However, it also remains to be determined whether the effects for icilin in macrophages are specific to TRPM8 only or whether icilin can exert effects on related family members such as TRPM2 and TRPV2.

Despite the detailed mechanism of the stimulatory action of icilin, our study also demonstrated that under current-clamp conditions this agent could depolarize the membrane in RAW 264.7 cells. Assuming that similar results observed in this study are found in macrophages in

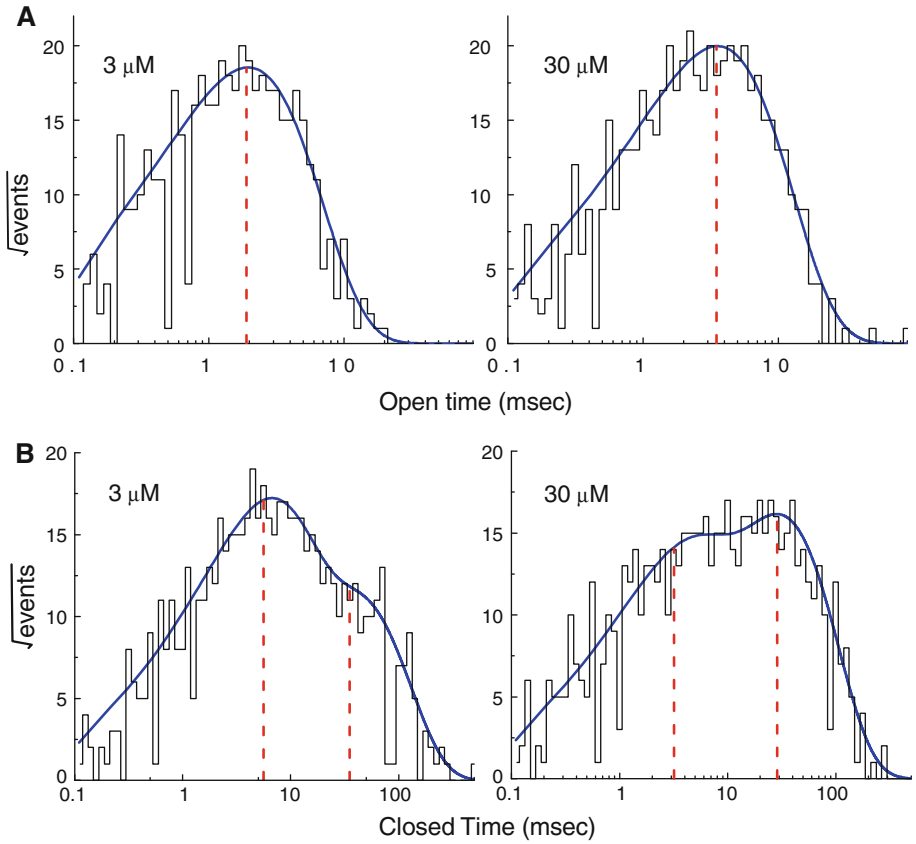

Fig. 6 Mean open (**a**) and closed (**b**) times of icilin-induced NS channels in RAW 264.7 cells. Open- and closed-time histograms obtained in the presence of 3 μM (*left*) and 30 μM (*right*) icilin are illustrated in **a** and **b**, respectively. Data were obtained from measurement of 96 channel openings with a total record time of 30 s in the presence of 3 μM icilin, whereas data were measured from 103 channel openings with a total record time of 20 s during exposure to 30 μM icilin. The abscissa and ordinate indicate the logarithm of open or closed time (ms) and the square root of the number of events, respectively. *Blue/smooth lines* shown in each lifetime distribution were fitted by one- or two-exponential function, whereas *red dashed lines* are placed at the value of the time constant. Notably, as the icilin concentration increases, there is both an increase in mean open time and a decrease in mean closed time (Color figure online)

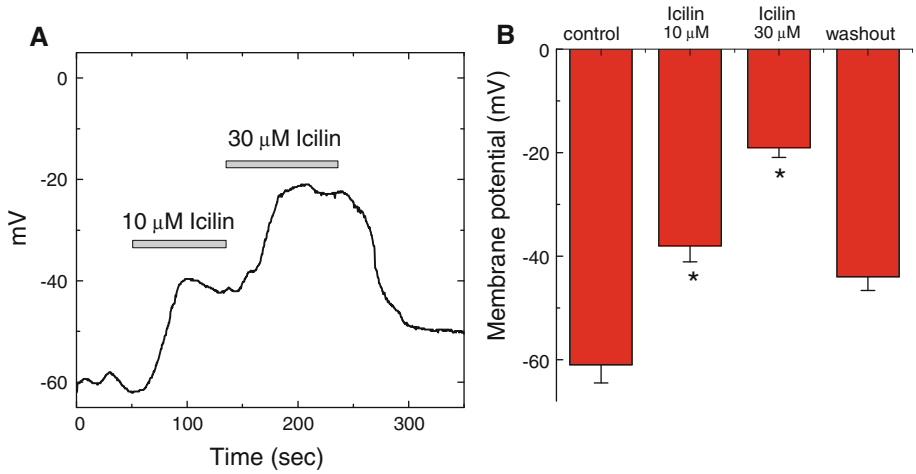

Fig. 7 Effect of icilin on the resting potential in RAW 264.7 cells. In these experiments, cells were bathed in normal Tyrode's solution containing 1.8 mM $CaCl_2$, the patch pipette was filled with K^+-containing solution and changes in the resting potential were measured under current-clamp configuration. **a** Potential trace showing the effect of icilin (10 and 30 μM) on membrane potential of a RAW 264.7 cell. Application of icilin indicated at the *horizontal bars* depolarizes the cell. **b** Bar graph showing summary of the effect of icilin (10 and 30 μM) on membrane potential in RAW 264.7 cells. Each bar represents mean ± SEM ($n = 6$–9). *Significantly different from control

vivo, ion flux through icilin-stimulated NS channels may underlie the mechanisms through which it influences their functional activities. Taken together, the present results provide further evidence for the existence of a novel non-neuronal cold temperature–elicited signal-transduction pathway in macrophages and support the hypothesis that this pathway may play a significant role in cold air–induced inflammation (Perraud et al. 2004; Miller 2006; Sabnis et al. 2008; Yamashiro et al. 2010).

Acknowledgments This work was partially aided by grants from the National Science Council (NSC-98-2320-B-006-MY3), Taiwan, through a contract awarded to S.-N. W. The authors thank Hsien-Ching Huang and Chia-Chen Yeh for technical assistance.

References

Carl A, Sanders KM (1990) Measurement of single channel open probability with voltage ramps. J Neurosci Methods 33:157–163

Channon JY, Leslie CC (1990) A calcium-dependent mechanism for associating a soluble arachidonoyl-hydrolyzing phospholipase A_2 with membrane in the macrophage cell line RAW 264.7. J Biol Chem 265:5409–5413

Chodon D, Guilbert A, Dhennin-Duthille I, Gautier M, Telliez MS, Sevestre H, Ouadid-Ahidouch H (2010) Estrogen regulation of TRPM8 expression in breast cancer cells. BMC Cancer 10:212

Chuang HH, Neuhausser WM, Julius D (2004) The super-cooling agent icilin reveals a mechanism of coincidence detection by a temperature-sensitive TRP channel. Neuron 43:859–869

Colburn RW, Lubin ML, Stone DJ Jr, Wang Y, Lawrence D, D'Andrea MR, Brandt MR, Liu Y, Flores CM, Qin N (2007) Attenuated cold sensitivity in TRPM8 null mice. Neuron 54:379–386

Fernández JA, Skryma R, Bidaux G, Magleby KL, Scholfield CN, McGeown JG, Prevarskaya N, Zholos AV (2011) Voltage- and cold-dependent gating of single TRPM8 ion channels. J Gen Physiol 137:173–195

Harteneck C (2005) Function and pharmacology of TRPM cation channels. Naunyn-Schmiedebergs Arch Pharmacol 371:307–314

Hui K, Guo Y, Feng Z-P (2005) Biophysical properties of menthol-activated cold receptor TRPM8 channels. Biochem Biophys Res Commun 333:374–382

Johnson CD, Melanaphy D, Purse A, Stokesberry SA, Dickson P, Zholos AV (2009) Transient receptor potential melastatin 8 channel involvement in the regulation of vascular tone. Am J Physiol Heart Circ Physiol 296:H1868–H1877

Kemmer G, Keller S (2010) Nonlinear least-squares data fitting in Excel spreadsheets. Nat Protocol 5:267–281

Kuo JH, Jan MS, Chang CH, Chiu HW, Li CT (2005) Cytotoxicity characterization of catanionic vesicles in RAW 264.7 murine macrophage-like cells. Colloids Surf B 41:189–196

Louhivuori LM, Bart G, Larsson KP, Louhivuori V, Näsman J, Nordström T, Koivisto A-P, Åkerman KE (2009) Differentiation dependent expression of TRPA1 and TRPM8 channels in IMR32 human neuroblastoma cells. J Cell Physiol 221:67–74

Mahieu F, Janssens A, Gees M, Talavera K, Nilius B, Voets T (2010) Modulation of the cold-activated cation channel TRPM8 by surface charge screening. J Physiol 588(2):315–324

McKemy DD, Neuhausser WM, Julius D (2002) Identification of a cold receptor reveals a general role for TRP channels in thermosensation. Nature 416:52–58

Mergler S, Strowski MZ, Kaiser S, Plath T, Giesecke Y, Neumann M, Hosokawa H, Kobayashi S, Langrehr J, Neuhaus P, Plöckinger U, Wiedenmann B, Grötzinger C (2007) Transient receptor potential channel TRPM8 agonists stimulate calcium influx and neurotensin secretion in neuroendocrine tumor cells. Neuroendocrinology 85:81–92

Miller BA (2006) The role of TRP channels in oxidative stress-induced cell death. J Membr Biol 209:31–41

Pan MH, Chang YH, Tsai ML, Lai CS, Ho SY, Badmaev V, Ho CT (2008) Pterostilbene suppressed lipopolysaccharide-induced up-expression of iNOS and COX-2 in murine macrophages. J Agric Food Chem 56:7502–7509

Parks DJ, Parsons WH, Colburn RW, Meegalla SK, Ballentine SK, Illig CR, Qin N, Liu Y, Hutchinson TL, Lubin ML, Stone DJ Jr, Baker JF, Schneider CR, Ma J, Damiano BP, Flores CM, Player MR (2011) Design and optimization of benzimidazole-containing transient receptor potential melastatin 8 (TRPM8) antagonists. J Med Chem 54:233–247

Perraud A-L, Knowles HM, Schmitz C (2004) Novel aspects of signaling and ion-homeostasis regulation in immunocytes. The TRPM ion channels and their potential role in modulating the immune response. Mol Immunol 41:657–673

Sabnis AS, Shadid M, Yost GS, Reilly CA (2008) Human lung epithelial cells express a functional cold-sensing TRPM8 variant. Am J Respir Cell Mol Biol 39:466–474

Sabovcik R, Li J, Kucera P, Prod'hom B (1995) Permeation properties of a Ca^{2+}-blockable monovalent cation channel in the ectoderm of the chick embryon: pore size and multioccupancy probed with organic cations and Ca^{2+}. J Gen Physiol 106:149–174

Sherkheli MA, Vogt-Eisele AK, Bura D, Beltrán Márgues LR, Gisselmann G, Hatt H (2010) Characterization of selective TRPM8 ligands and their structure activity response (S.A.R.) relationship. J Pharm Pharm Sci 13:242–253

Tominaga M, Caterina MJ (2004) Thermosensation and pain. J Neurobiol 61:3–12

Valero M, Morenilla-Palao C, Belmonte C, Viana F (2011) Pharmacological and functional properties of TRPM8 channels in prostate tumor cells. Pfluegers Arch 461:99–114

Wang H, Woolf CJ (2005) Pain TRPs. Neuron 46:9–12

Wondergem R, Bartley JW (2009) Menthol increases human glioblastoma intracellular Ca^{2+}, BK channel activity and cell migration. J Biomed Sci 16:90

Wu SN, Lin PH, Hsieh KS, Liu YC, Chiang HT (2003) Behavior of nonselective cation channels and large-conductance Ca^{2+}-activated K^+ channels induced by dynamic changes in membrane stretch in cultured smooth muscle cells of human coronary artery. J Cardiovasc Electrophysiol 14:44–51

Wu SN, Peng H, Chen BS, Wang YJ, Wu PY, Lin MW (2008) Potent activation of large-conductance Ca^{2+}-activated K^+ channels by the diphenylurea 1,3-bis-[2-hydroxy-5-(trifluoromethyl)phenyl]-urea (NS11643) in pituitary tumor (GH_3) cells. Mol Pharmacol 74:1696–1704

Yamashiro K, Sasano T, Tojo K, Namekata I, Kurokawa J, Sawada N, Suganami T, Kamei Y, Tanaka H, Tajima N, Utsunomiya K, Ogawa Y, Furukawa T (2010) Role of transient receptor potential vanilloid 2 in LPS-induced cytokine production in macrophages. Biochem Biophys Res Commun 398:284–289

Zakharian E, Cao C, Rohacs T (2010) Gating of transient receptor potential melastatin 8 (TRPM8) channels activated by cold and chemical agonists in planar lipid bilayers. J Neurosci 30:12526–12534

Zholos A (2010) Pharmacology of transient receptor potential melastatin channels in the vasculature. Br J Pharmacol 159:1559–1571